Dedicated Pinhole SPECT of Intestinal Neutrophil Recruitment in a Mouse Model of Dextran Sulfate Sodium–Induced Colitis

Roelof J. Bennink, MD, PhD[1]; Jörg Hamann, PhD[2]; Kora de Bruin[1]; Fiebo J.W. ten Kate, MD, PhD[3]; Sander J.H. van Deventer, MD, PhD[4]; and Anje A. te Velde, PhD[4]

[1]Department of Nuclear Medicine, Academic Medical Center, Amsterdam, The Netherlands; [2]Department of Clinical Immunology, Academic Medical Center, Amsterdam, The Netherlands; [3]Department of Pathology, Academic Medical Center, Amsterdam, The Netherlands; and [4]Department of Experimental Internal Medicine, Academic Medical Center, Amsterdam, The Netherlands

Evaluating the efficacy of therapy in experimental inflammatory bowel disease (IBD) requires information about inflammatory activity in bowel segments or leukocyte recruitment and about kinetics in the follow-up of treatment. This study evaluated a noninvasive scintigraphic technique able to assess neutrophil trafficking in a mouse model of dextran sulfate sodium (DSS)–induced colitis. **Methods:** Groups of 4 BALB/c mice were assessed at baseline and after 1, 3, 5, and 8 d of treatment with DSS. Donor neutrophils were harvested by rinsing of the peritoneal cavity with phosphate-buffered saline 5 h after intraperitoneal injection of proteose peptone contained in phosphate-buffered saline and labeled with freshly prepared ^{99m}Tc-hexamethylpropylene amine oxime (HMPAO). Pinhole SPECT of the abdomen was performed 1 h after reinjection of 50 MBq of labeled neutrophils. In addition, the severity of inflammation was determined by histologic examination. The possibilities of the technique were illustrated by scintigraphic assessment of neutrophil trafficking with and without blocking of neutrophil migration by a CD97 monoclonal antibody in mice with DSS-induced colitis. **Results:** Colonic uptake of ^{99m}Tc-HMPAO neutrophils was determined with dedicated animal pinhole SPECT in mice with DSS-induced colitis and correlated well with histologic findings ($R = 0.81$) and wet colon weight ($R = 0.87$) and moderately with clinical weight loss ($R = 0.62$). The neutrophil uptake ratio was reduced significantly ($P < 0.01$) by blocking of neutrophil migration capacity with the CD97 antibody. **Conclusion:** Animal pinhole SPECT can be used to study inflammatory activity and neutrophil recruitment in vivo in experimental colitis.

Key Words: ^{99m}Tc-HMPAO; pinhole SPECT; neutrophils; inflammatory bowel disease; dextran sulfate sodium colitis

J Nucl Med 2005; 46:526–531

Ulcerative colitis and Crohn's disease are chronic inflammatory bowel diseases (IBDs) characterized by periods of acute attacks and remission (1,2). Although the initiating events of IBD are still unknown, evidence is increasing that mucosal CD4$^+$ T cells activated by enteric bacteria initiate and perpetuate the inflammation in genetically susceptible individuals (3). Extravascular recruitment of neutrophils into the inflamed tissue plays a crucial role in the development of tissue damage (4). Molecular understanding of the mechanisms that guide leukocyte trafficking into the gut is rapidly increasing (5,6). This knowledge has led to the development of specific biologic therapies that mechanistically target individual inflammatory pathways (7,8). These designer drugs for IBD are created and subsequently tested for clinical potential (9).

A noninvasive technique able to assess inflammatory activity in bowel segments or leukocyte recruitment and kinetics in the follow-up of experimental treatment for IBD would not only benefit longitudinal studies but also reduce the number of animals required for testing (10). White blood cell scintigraphy, combining imaging of the affected colon with semiquantitative scoring of disease activity, can reliably and accurately determine the extent and intensity of ulcerative colitis lesions (11,12). Furthermore, white blood cell scintigraphy can monitor response to therapy at an early stage (13).

The mouse model of dextran sulfate sodium (DSS)–colitis reproduces many of the histopathologic and clinical features of acute colitis in humans (14) and is used for biologic evaluation of experimental treatment of IBD (15,16). Evaluation of inflammation and the effects of therapy implicates sacrificing the animal and prohibits a longitudinal study within the same animal.

Dedicated pinhole SPECT cameras can image radioactivity distribution in vivo in small animals with a spatial resolution on the order of a few millimeters (17,18). The system has been used successfully in experiments assessing lymphocyte homing in experimental colitis (19,20).

Therefore, the aim of this study was to construct and validate an animal model for IBD in which intestinal neutrophil recruitment can be monitored noninvasively in vivo by pinhole SPECT. To illustrate use of the technique for

imaging the effect of neutrophil migration modulation, we scanned DSS colitis mice after anti-CD97 monoclonal antibody blocking of neutrophil migration.

MATERIALS AND METHODS

Female BALB/c mice (8–10 wk old and weighing 20–25 g; Charles River) were housed and maintained under standard conditions at our animal care facility starting 1 wk before the experiments began. Food and water were given ad libitum. All animal experiments were performed with the approval and following the guidelines of the Animal Research Ethics Committee of the University of Amsterdam.

The study was divided into 2 experimental protocols. First, neutrophil recruitment in relationship to disease severity was assessed. Therefore, groups of 4 mice were scanned at baseline and after 1, 3, 5, and 8 d of treatment with DSS. The weight of each mouse was recorded on arrival and before scintigraphy. After scintigraphy, the mice were sacrificed and the colon was removed, measured, weighed, and processed for histologic examination. Second, as an example, neutrophil recruitment into the colon was assessed in 4 mice after blocking of neutrophil influx with an anti-CD97 monoclonal antibody (*21,22*). The neutrophils of control mice were incubated with a nonspecific control antibody. Mice were scanned 8 d after induction of colitis.

For injection and scintigraphy, each mouse was sedated by a single intraperitoneal administration of fentanyl and fluanisone (0.375 µg/g and 12 µg/g, respectively; Hypnorm; Janssen Pharmaceutica) and midazolam (6 µg/g; Roche). ^{99m}Tc-Neutrophils were administered by injection via the tail vein.

Mouse Model of DSS-Induced Colitis

DSS-induced acute colitis exhibits several morphologic and pathophysiologic features that resemble human colitis, including superficial ulceration, mucosal damage, production of cytokines and other inflammatory mediators, and leukocyte infiltration (*14*). The exact mechanism of induction and pathogenesis of DSS-induced colitis remain unknown. However, a direct toxic action on colonic epithelium, macrophage activation by DSS, and altered colonic microflora have all been implicated (*14,23*). Focal crypt lesions and secondary mucosal and submucosal inflammation with granulocytes and macrophages characterize the acute phase of DSS-induced colitis (*24*). Strain differences can influence the induction phase of DSS colitis; however, in BALB/c mice the disease is located mainly in the distal colon (*24*). For induction of DSS colitis, mice were continuously fed 4% (w/v) DSS (TdB Consultancy) in their drinking water until undergoing scintigraphy (*25*).

Peritoneal neutrophils were harvested in donor mice (BALB/c) by rinsing of the peritoneal cavity with 5 mL of sterile phosphate-buffered saline 5 h after intraperitoneal injection of 1 mL of 10% proteose peptone (Difco) in phosphate-buffered saline (*26*). We used 1 donor mouse for every DSS colitis mouse. For mice scanned on the same day, donor cells were pooled and together labeled to reduce the possibility of labeling variability and to reduce costs. A small sample of cells from the peritoneal exudate was analyzed by flow cytometry in a FACS (Becton Dickinson). Forward- and side-scatter properties were used to identify the neutrophils. Approximately 5×10^6 cells per mouse were harvested and labeled with freshly prepared ^{99m}Tc-hexamethylpropylene amine oxime (HMPAO) (*27*). After 15 min, the cells were washed and resuspended in 0.2 mL of saline. Approximately 50 MBq of ^{99m}Tc-HMPAO-labeled neutrophils were reinjected into a tail vein of mice with DSS colitis. For the blocking study, labeled neutrophils were incubated in vitro in saline containing 5 µg of aCD97 monoclonal antibody per milliliter for 15 min. Hamster immunoglobulin (Rockland) was used as a control.

Camera Design

For imaging small laboratory animals, a previously described high-resolution pinhole SPECT technique was used (*18*). Briefly, we used a mechanism in which the gantry and the collimator were fixed and the animal rotated. The animal was fixed in an acrylic cylinder mounted on a step motor–driven system and positioned exactly above the pinhole collimator of a γ-camera. The step motor was controlled by a HERMES acquisition and processing system (Nuclear Diagnostics). After each projection had been acquired, a signal was given to rotate the step motor to the desired number of angular degrees. The system allowed adjustment of the radius of rotation and adjustment along the axis of the cylinder to select the field of view. The mechanical support was designed such that the midline of the cylinder was exactly in the middle of the pinhole. The SPECT acquisition could thus be regarded as a conventional circular orbit acquisition with a rotating camera head.

Scintigraphy and Interpretation

An ARC3000 scintillation camera (Philips) was used with a circular field of view of 400-mm diameter. The pinhole collimator had a diameter of 300 mm and an opening angle of 60°. A tungsten pinhole insert of 3-mm aperture was used. All studies were acquired with a 15% energy window on the ^{111}In 173- and 247-keV photopeaks. A HERMES workstation was used to control both the camera and the step motor.

The SPECT acquisition was performed 1 h after intravenous injection of neutrophils. Immediately before scintigraphy, the urinary bladder was emptied by manual compression. Fifty projections (25 s per view, 64 × 64 matrix) were made in a 360° orbit. Reconstruction was performed using a HERMES application program adapted to pinhole SPECT, with filtered backprojection (*18*) and a Butterworth filter (order, 5; 0.8 cycles/cm).

To determine the uptake ratio, we selected and summed the 5 consecutive transverse slices with the highest colon uptake for each mouse. Regions of interest were set for the colon and for abdominal background adjacent to the colon. The colon uptake ratio was calculated by subtracting background activity from colon activity and subsequently dividing the corrected colon uptake by the background activity to yield a specific uptake ratio: (counts colon −background counts)/background counts.

Histologic Examination

After scintigraphy, the animals were sacrificed by cervical dislocation, and the colons were removed through a laparotomy and opened through a midline incision. The isolated colons were rinsed with saline. The wet weight of each colon was recorded and used as an index of disease-related intestinal wall thickening. An experienced pathologist microscopically evaluated formalin-fixed hematoxylin- and eosin-stained tissue sections in a masked fashion. Two sections of rolled colon were evaluated, and grading from 0 to 26 points was used to indicate the incidence and severity of inflammatory lesions based on the extent of the involved area, the number of follicle aggregates, edema, fibrosis, erosion/ulceration, crypt loss, and infiltration of mononuclear or polymorphonuclear cells (*25*).

TABLE 1
Experiment 1: Characteristics

Group	DSS (d)	Weight loss (g)	Colon weight (g/cm, ×100)	Histologic score	Scintigraphic uptake ratio
A	1	0.00 ± 0.07	1.045 ± 0.005	0.37 ± 0.13	1.11 ± 0.02
B	3	0.08 ± 0.11	1.053 ± 0.046	3.25 ± 0.52*	1.21 ± 0.17
C	5	1.17 ± 0.11*	1.170 ± 0.105	8.13 ± 1.23*	1.96 ± 0.21
D	8	1.98 ± 0.62*	1.993 ± 0.137*	17.17 ± 0.60*	5.40 ± 1.58*

*$P < 0.05$.

Statistical Analysis

Values are given as mean and SEM per treatment group. Changes in weight and in histologic and scintigraphic characteristics over time were analyzed by 1-way ANOVA. Differences between 2 groups were analyzed by the nonparametric Mann–Whitney U test. All statistical tests were 2-tailed, and differences were evaluated at the 5% level of significance.

RESULTS

Clinical and Pathologic Parameters

The weight of the mice before they entered the trial was 22.83 ± 0.26 g. The mice were randomly assigned to 4 groups (groups A–D) and treated with DSS for 1–8 d (Table 1). There was a significant loss of weight after 5 and 8 d of DSS ($P < 0.01$; Fig. 1A). After resection and cleaning of the resected colon, the colon weight (g/cm) was found to have increased with increasing duration of DSS administration. There was a significant increase in colon weight after 8 d ($P < 0.05$; Fig. 1B). The histologic score increased significantly with increasing duration of DSS administration ($P < 0.01$; Fig. 2A).

Scintigraphy

The percentage of neutrophils in the peritoneal lavage fluid was 90% of peritoneal exudate cells. The radiochemical purity of ^{99m}Tc-HMPAO was greater than 95%. Cell labeling was reproducible. The labeling efficiency of neutrophils was enough for pinhole SPECT. An average of 6.0 ± 0.6 × 10^6 cells containing 52.9 ± 4.8 MBq of ^{99m}Tc-HMPAO in 0.2 mL was reinjected into a tail vein without clinical consequences. There was no bowel uptake of any significance 1 h after reinjection of labeled cells in control animals (mean uptake ratio, 0.11 ± 0.02).

Neutrophil Recruitment in Relation to Disease Severity. Figure 3 shows transverse SPECT slices at various durations of DSS administration. The colonic uptake of labeled cells was clearly visible, besides physiologic uptake in bone marrow. Other physiologic uptake such as in the kidney and urinary bladder did not cause any practical problems on SPECT acquisitions. ^{99m}Tc-HMPAO–labeled neutrophil uptake in the colon increased with time (Fig. 2B). The uptake was significantly higher ($P < 0.01$) after 5 and 8 d of DSS administration than in controls. The scintigraphic uptake ratio correlated well with the histologic score of inflammation ($R = 0.81$) and the wet weight of the resected and cleaned colon specimens ($R = 0.87$) and moderately with clinical weight loss ($R = 0.62$).

Blocking Experiment. The mice, research circumstances, and procedures for the blocking experiment were identical to those for the first experiment. DSS was administered for 8 d before scintigraphy. In mice with DSS-induced colitis, the uptake ratio of labeled neutrophils incubated with the control antibody was not significantly different from that of untreated neutrophils (4.00 ± 1.05 and 5.40 ± 1.58, respectively). After neutrophil migration had been blocked with the aCD97 monoclonal antibody, the uptake ratio of ^{99m}Tc-HMPAO–labeled neutrophils was significantly decreased (1.16 ± 0.26, $P < 0.01$; Figs. 4 and 5).

DISCUSSION

DSS is a heparinlike polysaccharide containing up to 3 sulfate groups per glucose molecule. Depending on the time course of oral administration in the drinking water, DSS can induce in mice both acute and chronic colitis that exhibits

FIGURE 1. First experiment. (A) Bar graph showing mean loss of body weight (+SEM) for mice treated 1, 3, 5, and 8 d with 4% (w/v) DSS in their drinking water. Weight loss after 5 and 8 d of DSS administration is significant ($P < 0.01$). (B) Bar graph showing mean increase in wet colon weight (+SEM) for mice treated 1, 3, 5, and 8 d with 4% (w/v) DSS in their drinking water. Weight increase after 8 d of DSS administration is significant ($P < 0.05$).
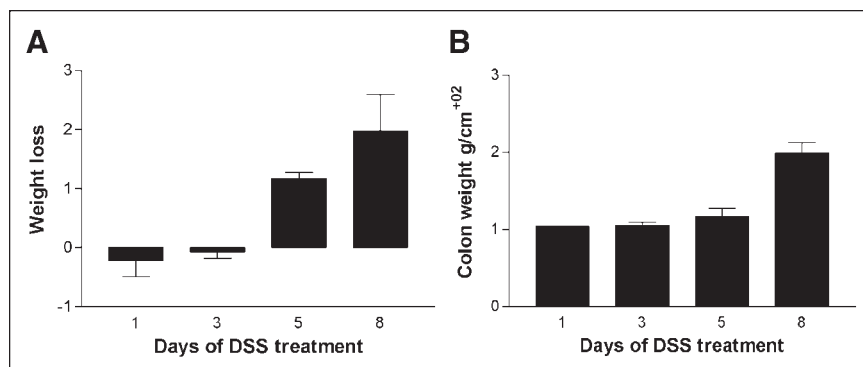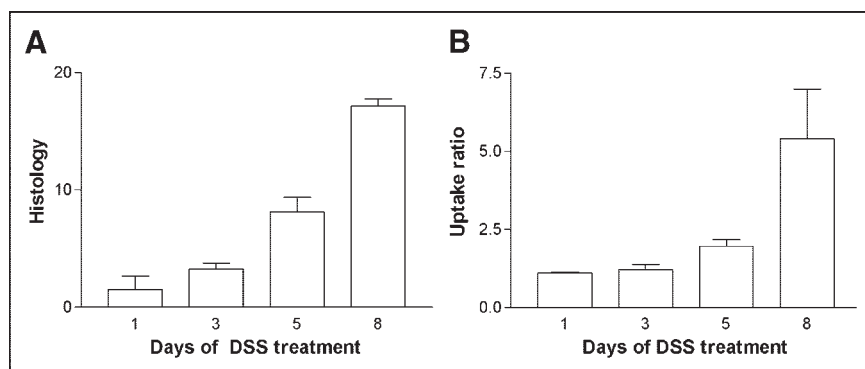
FIGURE 2. First experiment. (A) Bar graph showing histologic score of colon resection specimens (+SEM) for mice treated 1, 3, 5, and 8 d with 4% (w/v) DSS in their drinking water. Increase after 5 and 8 d of DSS administration is significant ($P < 0.01$). (B) Bar graph showing increase in scintigraphic uptake ratio (+SEM) for mice treated 1, 3, 5, and 8 d with 4% (w/v) DSS in their drinking water. Increase in colon uptake ratio of neutrophils after 8 d of DSS administration is significant ($P < 0.05$).

several morphologic and pathophysiologic features resembling human colitis (*23*). This model has proved useful for examining fundamental mechanisms underlying the inflammatory pathophysiology associated with IBD and for screening potential therapeutic interventions (*15,23*). In our series, induction of acute colitis was successful and reproducible. This is not, however, always the case, since susceptibility and responsiveness to DSS differ with the strain of the mouse, the concentration and molecular weight of the DSS, and the duration of exposure to it (*23*). The exact mechanism of induction and pathogenesis of DSS-induced colitis is unknown. A direct toxic action on colonic epithelium, macrophage activation by DSS, and altered colonic microflora have all been implicated (*23*). Histologically, the colon shows inflammatory cell infiltration that includes neutrophils and mononuclear cells (*24*).

Large amounts of polymorphonuclear neutrophils can be harvested from the murine abdominal cavity 3 h after an intraperitoneal injection of proteose peptone (*26*). We obtained an average of 6×10^6 cells/mL, a number that is not different from numbers reported in the literature (*26*). Increasing the number of donor mice to increase the number of cells for labeling is a possibility. However, labeled cells have to be reinjected into a tail vein of a recipient mouse, limiting cell suspension viscosity and the volume injected to a maximum of 0.2 mL. Cells were labeled with ^{99m}Tc-HMPAO. Compared with ^{111}In-oxinate, use of ^{99m}Tc-HMPAO as a label has the advantages of greater availability, superior imaging characteristics, and superior biologic properties but is less efficient (*28*). Labeling efficiency can be maximized using freshly prepared ^{99m}Tc-HMPAO with the highest possible specific activity and in our experiments was good. An average yield of 9.2 MBq per 10^6 cells is superior to the average yield in clinical practice (*28*). Reporting a labeling efficiency based on radioactivity counting of the cell pellet and supernatant would not be appropriate, since a maximal dose of ^{99m}Tc-HMPAO with highest spe-
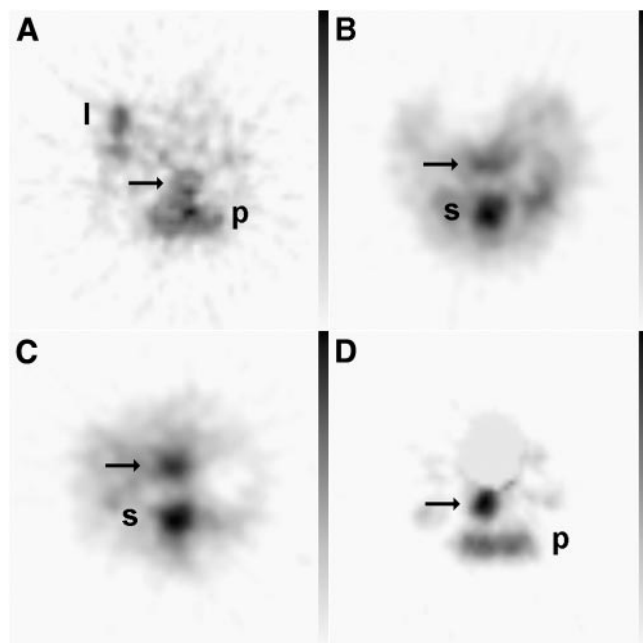

FIGURE 3. First experiment. Images are representative transverse pinhole SPECT slices of abdomen of mice treated for 1 d (A), 3 d (B), 5 d (C), and 8 d (D) with 4% (w/v) DSS in their drinking water. Increasing uptake of ^{99m}Tc-HMPAO–labeled neutrophils is seen in colon (arrows). Physiologic uptake of activity is seen in bone marrow of pelvis (p), spine (s), or limbs (l). Activity in urinary bladder (D) has been masked.
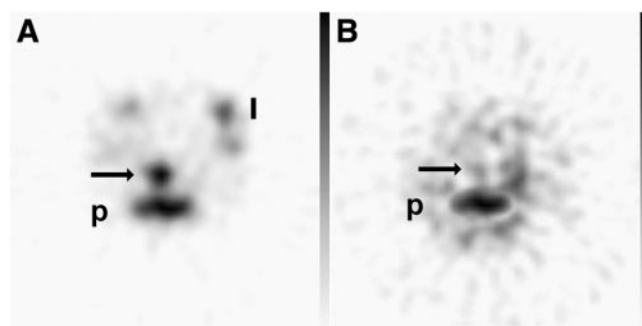

FIGURE 4. Second experiment. Images are representative transverse pinhole SPECT slices of abdomen of mice treated for 8 d with 4% (w/v) DSS and injected with labeled neutrophils incubated with control antibody (A) or with aCD97 (B). Significant decrease in uptake of ^{99m}Tc-HMPAO–labeled neutrophils is seen in colon of mice with aCD97-blocked neutrophil migration (arrow, B). Physiologic uptake of activity is seen in bone marrow of pelvis (p) or limbs (l).
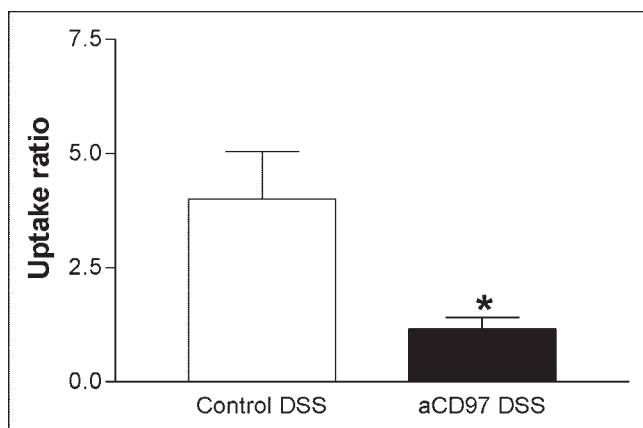
FIGURE 5. Second experiment. Bar graph shows mean scintigraphic uptake ratio (+SEM) of labeled neutrophils in mice treated for 8 d with 4% (w/v) DSS in their drinking water. Uptake is significantly lower ($P < 0.01$) after blocking of neutrophil migration with aCD97 antibody than after aspecific control antibody.

cific activity in a minimal volume exceeding by far the volume containing the limited number of cells has no additional value.

An average of 53 MBq of ^{99m}Tc-HMPAO in 6×10^6 cells was sufficient for pinhole SPECT 1 h after reinjection. This timing was based on knowledge of physiologic cell migration, with initial lung retention and possible physiologic bowel excretion of label over time (27,29,30). Image acquisition and reconstruction proved feasible using a methodology comparable to that used for imaging of lymphocyte homing (20). The use of ^{99m}Tc-HMPAO instead of ^{111}In-oxinate is associated with physiologic uptake and excretion in the urinary system and the secondary possible reconstruction or contamination artifacts. Manual bladder emptying before scintigraphy, however, minimized the magnitude of this problem.

The presence of leukocytes in the colon can be determined visually and, by means of an uptake ratio, semiquantitatively on transverse SPECT slices. The uptake ratio of colon to surrounding tissue eliminates variables dependent on the exact amount of radioactivity injected intravenously and normalizes subjects within and between groups. Neutrophil uptake in the colon increased with increasing duration of DSS administration, as was consistent with the described DSS colitis model (23). The close correlation between scintigraphic uptake, clinical (body weight) parameters, and pathologic parameters demonstrates that pinhole SPECT can be used as a noninvasive imaging tool to assess intestinal inflammation in this murine colitis model.

CD97 is a member of the epidermal growth factor 7 transmembrane family. It is found on granulocytes with high expression at sites of inflammation (22). CD97 plays a role in the onset of protective as well as destructive immune responses and is believed to play an essential role in the migration of neutrophils (22). By blocking this receptor

with an anti-CD97 monoclonal antibody, we were able to illustrate the application of leukocyte scintigraphy in the DSS colitis model. When a nonspecific immunoglobulin was used as a control, neutrophil uptake was not different from the model validated in the first experiment.

Looking at our results, one could state that histology is more sensitive than scintigraphy for the assessment of disease severity. However, detection of colitis is not the only issue. The purpose of the DSS colitis model is to assess experimental treatment on induced colitis. Therefore, colitis has to be induced, and this induction is known to be dependant on multiple factors, influencing the induction time needed (23). Currently, weight loss is the noninvasive parameter used most frequently to estimate the success of induction of colitis. However, weight loss is a secondary parameter, which will be replaced by histology at the end of the experiment. Scintigraphy is able to quantify the severity of induced colitis and assess the effect of therapy within the same animal without the need to sacrifice the animal, making repetitive assessment possible.

The recognition of cellular messengers, including nuclear factors, cytokines, chemokines, and adhesion molecules, offers novel targets for therapy of IBD (31). Antiinflammatory strategies based on blunting the multistep adhesion cascade of lymphocytes to reduce aberrant homing have been proposed (5,8,9). For in vivo evaluation of these strategies, most preclinical studies have involved animal dissection and histologic examination. Preclinical studies using radioisotopes have involved either animal dissection and specimen counting or autoradiography, since image resolution obtained using conventional γ-camera techniques has been less than optimal for small laboratory animals. Therefore, prepharmacologic and postpharmacologic studies could not be performed on the same animal (10). White blood cell pinhole SPECT of mice, besides being used to evaluate lymphocyte homing (20), can now be used to noninvasively evaluate experimental biologic IBD therapy aimed at decreasing neutrophil recruitment into inflamed tissue.

CONCLUSION

The data presented here show that dedicated animal pinhole SPECT can be used to study neutrophil homing in vivo in experimental colitis. Migration of neutrophils isolated from donor mice to the inflamed intestine could be detected 1 h after injection of labeled cells by visual analysis and calculation of the radioactivity uptake ratio. The possibility of assessing the intensity of inflammation in vivo before and after treatment in this model is interesting for longitudinal studies of the efficacy of novel treatment strategies in IBD and will reduce the number of animals needed.

REFERENCES

1. Podolsky DK. Inflammatory bowel disease (1). *N Engl J Med.* 1991;325:928–937.
2. Langholz E, Munkholm P, Davidsen M, Binder V. Course of ulcerative colitis:

analysis of changes in disease activity over years. *Gastroenterology.* 1994;107: 3–11.

3. Fiocchi C. Inflammatory bowel disease: etiology and pathogenesis. *Gastroenterology.* 1998;115:182–205.

4. Weiss SJ. Tissue destruction by neutrophils. *N Engl J Med.* 1989;320:365–376.

5. Salmi M, Jalkanen S. Molecules controlling lymphocyte migration to the gut. *Gut.* 1999;45:148–153.

6. Sun FF, Lai PS, Yue G, et al. Pattern of cytokine and adhesion molecule mRNA in hapten-induced relapsing colon inflammation in the rat. *Inflammation.* 2001; 25:33–45.

7. Sandborn WJ, Targan SR. Biologic therapy of inflammatory bowel disease. *Gastroenterology.* 2002;122:1592–1608.

8. Lim WC, Hanauer SB. Emerging biologic therapies in inflammatory bowel disease. *Rev Gastroenterol Disord.* 2004;4:66–85.

9. Bruno O, Brullo C, Arduino N, et al. Synthesis and biological evaluation of neutrophilic inflammation inhibitors. *Farmaco.* 2004;59:223–235.

10. Weber DA, Ivanovic M. Ultra-high-resolution imaging of small animals: implications for preclinical and research studies. *J Nucl Cardiol.* 1999;6:332–344.

11. Guimbaud R, Beades E, Chauvelot-Moachon L, et al. Technetium Tc 99m hexamethyl propylene amine oxine leukocyte scintigraphy in patients with ulcerative colitis: correlation with clinical, biologic, endoscopic, and pathologic intensity, and local release of interleukin 8. *Gastrointest Endosc.* 1998;48:491–496.

12. Bennink RJ, Peeters M, D'Haens G, Rutgeerts P, Mortelmans L. Tc99m-HMPAO WBC scintigraphy in the assessment of the extent and severity of an acute exacerbation of ulcerative colitis. *Clin Nucl Med.* 2001;26:99–104.

13. Bennink RJ, Peeters M, Rutgeerts P, Mortelmans L. Evaluation of early treatment response and predicting the need for colectomy in active ulcerative colitis with 99mTc-HMPAO white blood cell scintigraphy. *J Nucl Med.* 2004;45:1698–1704.

14. Okayasu I, Hatakeyama S, Yamada M, Ohkusa T, Inagaki Y, Nakaya R. A novel method in the induction of reliable experimental acute and chronic ulcerative colitis in mice. *Gastroenterology.* 1990;98:694–702.

15. Vowinkel T, Mori M, Krieglstein CF, et al. Apolipoprotein A-IV inhibits experimental colitis. *J Clin Invest.* 2004;114:260–269.

16. Vandenbroucke K, Hans W, Van Huysse J, et al. Active delivery of trefoil factors by genetically modified Lactococcus lactis prevents and heals acute colitis in mice. *Gastroenterology.* 2004;127:502–513.

17. Strand SE, Ivanovic M, Erlandsson K, et al. Small animal imaging with pinhole single-photon emission computed tomography. *Cancer.* 1994;73:981–984.

18. Habraken JB, de Bruin K, Shehata M, et al. Evaluation of high-resolution pinhole SPECT using a small rotating animal. *J Nucl Med.* 2001;42:1863–1869.

19. van Montfrans C, Bennink RJ, de Bruin K, et al. In vivo evaluation of 111In-labeled T-lymphocyte homing in experimental colitis. *J Nucl Med.* 2004;45: 1759–1765.

20. Bennink RJ, van Montfrans C, de Jonge WJ, de Bruin K, Van Deventer SJ, te Velde AA. Imaging of intestinal lymphocyte homing by means of pinhole SPECT in a TNBS colitis mouse model. *Nucl Med Biol.* 2004;31:93–101.

21. Kwakkenbos MJ, Kop EN, Stacey M, et al. The EGF-TM7 family: a postgenomic view. *Immunogenetics.* 2004;55:655–666.

22. Leemans JC, te Velde AA, Florquin S, et al. The epidermal growth factor-seven transmembrane (EGF-TM7) receptor CD97 is required for neutrophil migration and host defense. *J Immunol.* 2004;172:1125–1131.

23. Vowinkel T, Kalogeris TJ, Mori M, Krieglstein CF, Granger DN. Impact of dextran sulfate sodium load on the severity of inflammation in experimental colitis. *Dig Dis Sci.* 2004;49:556–564.

24. Dieleman LA, Palmen MJ, Akol H, et al. Chronic experimental colitis induced by dextran sulphate sodium (DSS) is characterized by Th1 and Th2 cytokines. *Clin Exp Immunol.* 1998;114:385–391.

25. Ten Hove T, Drillenburg P, Wijnholds J, te Velde AA, Van Deventer SJ. Differential susceptibility of multidrug resistance protein-1 deficient mice to DSS and TNBS-induced colitis. *Dig Dis Sci.* 2002;47:2056–2063.

26. Miyazaki S, Ishikawa F, Fujikawa T, Nagata S, Yamaguchi K. Intraperitoneal injection of lipopolysaccharide induces dynamic migration of Gr-1(high) polymorphonuclear neutrophils in the murine abdominal cavity. *Clin Diagn Lab Immunol.* 2004;11:452–457.

27. Welling M, Feitsma HI, Blok D, et al. A new 99mTc labelling method for leucocytes: in vitro and in vivo comparison with 99mTc-HMPAO. *Q J Nucl Med.* 1995;39:89–98.

28. Stoeckli TC, Zimmerli W, Maecke HR, Fridrich R. Comparison of chemotaxis and superoxide generation of indium-111-oxine- and technetium-99m-HMPAO-labelled granulocytes. *Scand J Clin Lab Invest.* 1996;56:305–309.

29. Babbar A, Mishra P, Chauhan UP. A novel method for labelling of leukocytes with technetium-99m and its comparative evaluation for abscess scintigraphy. *Int J Rad Appl Instrum B.* 1988;15:689–694.

30. Weldon MJ. 99mTc-HMPAO planar white cell scanning. *Scand J Gastroenterol Suppl.* 1994;203:36–42.

31. Sands BE. Biologic therapy for inflammatory bowel disease. *Inflamm Bowel Dis.* 1999;3:95–113.